Transactive Energy Framework in Multi-Carrier Energy Hubs: A Fully Decentralized Model

Mohammad Sadegh Javadi [1*], Ali Esmaeel Nezhad [2*], Ahmad Rezaee Jordehi [3],

Matthew Gough [1,4], Sérgio F. Santos [1] and João P. S. Catalão [1,4]

[1] Institute for Systems and Computer Engineering, Technology and Science (INESC TEC), Porto, Portugal

[2] Department of Electrical Engineering, School of Energy Systems, LUT University, 53850, Lappeenranta, Finland

[3] Department of Electrical Engineering, Rasht Branch, Islamic Azad University, Rasht, Iran

[4] Faculty of Engineering of the University of Porto, (FEUP), Porto, Portugal

* Corresponding Authors: msjavadi@gmail.com and Ali.esmaeelnezhad@gmail.com

Abstract: This paper investigates a fully decentralized model for electricity trading within a transactive energy market. The proposed model presents a peer-to-peer (P2P) trading framework between the clients. The model is incorporated for industrial, commercial, and residential energy hubs to serve their associated demands in a least-cost paradigm. The alternating direction method of multipliers (ADMM) is implemented to address the decentralized power flow in this study. The optimal operation of the energy hubs is modeled as a standard mixed-integer linear programming (MILP) optimization problem. The corresponding decision variables of the energy hubs operation are transferred to the peer-to-peer (P2P) market, and ADMM is applied to ensure the minimum data exchange and address the data privacy issue. Two different scenarios have been studied in this paper to show the effectiveness of the electricity trading model between peers, called integrated and coordinated operation modes. In the integration mode, there is no P2P energy trading while in the coordinated framework, the P2P transactive energy market is taken into account. The proposed model is simulated on the modified IEEE 33-bus distribution network. The obtained results confirm that the coordinated model can efficiently handle the P2P transactive energy trading for different energy hubs, addressing the minimum data exchange issue, and achieving the least-cost operation of the energy hubs in the system. The obtained results show that the total operating cost of the hubs in the coordinated model is lower than that of the integrated model by $590.319, i.e. 11.75% saving in the costs. In this regard, the contributions of the industrial, commercial, and residential hubs in the total

cost using the integrated model are $3441.895, $596.600, and $988.789, respectively. On the other hand, these energy hubs contribute to the total operating cost in the coordinated model by $2932.645, $590.155, and $914.165 respectively. The highest decrease relates to the industrial hub by 14.8% while the smallest decrease relates to the residential hub by 1%. Furthermore, the load demand in the integrated and coordinated models is mitigated by 13% and 17%, respectively. These results indicate that the presented framework could effectively and significantly reduce the total load demand which in turn leads to reducing the total cost and power losses.

Keywords: Alternating Direction Method of Multipliers, Peer-to-Peer, Transactive Energy, Multi-Carrier Energy Hubs.

1- Introduction

A. Motivation

Emerging local generation technologies at load centers can provide considerable flexibility for prosumers and grid operators [1]. In this paradigm, serving the local electrical, heating, and cooling loads at the minimum cost is achievable through multi-carrier energy hubs. The main functionality of the energy hubs is to serve the consumer's loads within the utilization area. Various technologies are used for converting, storing, and generating energy in the hubs to serve the end-users' demands. In this regard, the energy hub operator is responsible for determining the optimal operating points of the installed assets in the hub. Unlike classic consumers, the energy hub operators can sell their surplus electricity to the upstream grid and as a result, they become prosumers in this paradigm since they can act as a producer as well as a consumer in the market [2]. This possibility for the prosumers can increase the flexibility of the energy hub operator in the market. On the other hand, the possibility of energy tradings between the clients in the P2P framework opens a new window for the end-users to trade electricity in a secure and least-cost model. In this environment, the clients can participate in a transactive energy market and benefit from this possibility to reduce their electricity cost by satisfying their energy needs from other energy hubs and increasing their benefits by selling their surplus power to other clients while avoiding paying extra tax or grid service costs. This paper investigates the

energy transactions between the energy hubs considering a transparent market mechanism for energy trading while addressing the minimum data exchange between the clients using the alternating direction method of multipliers (ADMM) based optimal power flow (OPF), known as the ADMM-OPF approach [3].

B. Literature Review

The problem of optimal operation of energy hubs has recently captured significant attention. There has been much research using a centralized framework to minimize the total operating costs while still supplying the required electrical, heating, and cooling demands. Also, multi-carrier energy systems using electricity and natural gas (NG) can be utilized. In this respect, combined heat and power (CHP) units could significantly improve the efficiency of the energy hub. This generation technology, besides the multi-carrier feature, would help provide the required flexibility to meet the load demand. In general, the studies carried out on energy hubs are categorized into two groups, either optimal management of energy hubs [4] or the optimal sizing of the hubs' assets [5]. The problem of optimal operation of hubs is characterized mainly by using matrix-based or energy flow models. The energy flow models enable the system operator to efficiently apply the dynamic behavior of energy storage systems, either thermal or electrical, to the hub. The optimal operation of multiple interconnected energy hubs has been investigated in the context of microgrid (MG) operation. The resulting problem will be large if the number of hubs is considerable.

Ref. [6] proposed a new steady-state methodology for the optimal energy management of energy hubs, helping overcome the existing restrictions of prevailing energy hub management models. In this respect, a graph theory-based technique was used for the steady-state study of the system for certain operational scenarios of the MG.

A centralized operation framework has been developed in [7], with the aim to minimize the operating cost of the system while addressing the constraints of the energy hub. The system has been studied using an ACOPF tool to take into consideration the reactive power and voltage security of the system.

The problem has been formulated as a mixed-integer linear programming (MILP) problem and presented to promote the efficiency and robustness of the system's day-ahead operation. The robust scheduling of combined cooling, heat, and power energy hubs in the presence of uncertainties of demands, photovoltaic (PV) systems, and wind power generation, as well as electricity price, has been addressed in [8]. The risk-aware scheduling model has been developed based on the information gap decision theory approach. The reported results illustrate that the sensitivity of the energy hub operating cost may be very different with respect to different sets of uncertain input data. The findings also show the significant effect of risk-awareness on the schedule of the hub components and its operation cost.

Another centralized model for the day-ahead operation of multi-carrier energy systems has been introduced in [9] aimed at minimizing the daily operating cost of the entire network. The nodal energy flow model for multi-energy carries has been investigated for MGs. The impacts of electric vehicles and parking lots on the day-ahead scheduling of a specific energy hub have been considered in [10] while the benefits of demand response programs have been demonstrated.

The optimal operation of a system with multiple MGs, including generation and storage technologies, has been addressed in [11] which uses a distributed stochastic framework with the least data exchange possible. In this regard, the resources of every MG are individually dispatched and the operation of each MG is coordinated with the operation of other MGs to make the most of the capabilities of such systems and maximize their social benefits. It is noteworthy that the Lagrangian dual method has been deployed for decentralizing the above-mentioned problem to enhance the system operation. Another piece of research investigated the reserve allocation for multi-area energy networks by implementing a chance-constrained optimization framework, handling the risks caused by electricity and NG systems [12]. By using the presented model, the first problem with a centralized structure is transformed into various sub-problems for each area to solve individually. This technique would help promote the protection of information for each area. Moreover, the distributed problem is tackled by

utilizing the ADMM method which is further improved by the use of self-adaptive penalty parameters. By setting a pre-defined confidence level, a probabilistic tool was employed to satisfy the electricity and NG systems' required reserve limitations.

The problem of optimal operation of multiple meshed MGs with interconnected energy hubs has been formulated as a distributed robust optimization problem in [13]. The developed framework is subject to the constraints of the MGs and gives a decentralized operational strategy while taking into account the ownership issues of energy suppliers. In this relation, the ADMM technique is deployed to enhance the data protection of the individual energy management systems.

Regarding the ADMM implementation for addressing data-privacy concerns, a comprehensive model has been introduced in [14] investigating a carbon emission trading system for power systems with considerable wind power generation. The proposed ADMM model has been implemented based on the finite-time average consensus algorithm reported in [3] dealing with sharing consensus variables between nodes. Furthermore, different graph topologies have been examined in [15] to validate the effectiveness and robustness of the algorithm.

A similar approach has been presented in [16] to address the optimal power flow with carbon emission trading based on the DCOPF framework in a centralized fashion. It is worth mentioning that transactive energy trading between end-users and small-scale prosumers not only occupies the distribution assets capacity but also introduces unknowns to utilities from a financial viewpoint leading to numerous issues. The first concern is that the income of the electrical utility decreases as a result of reduced energy delivered to its customers due to transactive energy trading amongst the customers. In addition, all energy transactions should respect the constraints of the distribution system and in this respect, two different strategies have been suggested in [17] as peer-centric and centralized strategies. By using the centralized framework, the system operation and transactive transactions are coordinated. The peer-centric methodology would not take the utility into consideration. It is also

noteworthy that the locational marginal prices are used to determine the network costs to pay to the utility.

Ref. [18] proposes a multi-bilateral economic dispatch model for a transactive market mechanism, providing the opportunity for multi-bilateral trading with product differentiation. An innovative relaxed consensus technique is proposed to tackle the problem within the decentralized framework. The framework resulted in the optimal solution while addressing the requirements of the consumers to maximize social welfare. A new optimization method based on the primal-dual gradient has been suggested in [19] for decentralized market clearing while disregarding any intervention by a central entity. The model takes into account the network constraints to allow for valid bidirectional energy trading while satisfying the consumers' requirements. The mechanisms of transactive energy trading have been extensively reviewed in [20] and the practical prospects of transactive energy trading have been investigated in [21]. Regarding the implementation of a P2P energy trading mechanism in energy hubs, preliminary research has been conducted in [22]. An effective transactive energy trading mechanism has been developed which allows for multi-hub coordinated operation with enhanced performance through the use of an efficient self-adjusted trading mechanism for the hubs. A general scheme has also been designed for the transactive energy prices, initially incorporated into an enhanced ADMM technique in order to reach the consensus of the P2P transaction between energy hubs. However, this paper neglected the network constraints, solution feasibility, and data privacy issue.

Energy hubs within networked microgrids were investigated by [23] to meet the demand for various energy carriers. The authors used the ADMM to optimally schedule power exchanges between the various microgrids and the distribution network. The authors considered a robust optimization model to account for the various uncertainties in the model and compared the results to those reported by heuristic algorithms. The optimal solution from the ADMM model was superior compared to those obtained from the heuristic algorithms. An ADMM-based planning model considering both energy

hubs using electricity and natural gas was developed in [24]. The authors incorporated a unit commitment model into the planning model to better reflect the operational strategies. The energy flows between the energy hubs and the networks were defined as continuous coupling variables for updating the Lagrange multipliers in the ADMM model. A distributed auction mechanism for energy hubs was developed in [25]. The energy hubs served a variety of building users and used their expected demand profiles as the basis for the auction mechanism. The auction mechanism was shown to achieve the incentive compatibility in a Nash equilibrium and also to be robust against any manipulations by the users. The paper only considered residential users in the model. A model predictive control (MPC)-based model was presented in [26] for the optimal energy management of hybrid electric vehicles. The authors used the ADMM and compared its performance with the dynamic programming (DP). Results showed that the ADMM had a lower solution time with comparable accuracy in comparison with the DP. A decentralized transactive energy management framework was developed in [22]. This framework allowed for the coordination between multiple energy hubs to improve the financial performance of the system. The authors considered the peer-to-peer trading possibility within the energy hubs. This was carried out by using the ADMM to achieve consensus regarding the trades within the energy hubs. Results showed that consumers are encouraged to engage in the energy hubs activities. The demand response programs were not considered in this model. A large-scale energy hub was developed by [27]. This model was designed to coordinate energy flows between nations or large regions. The authors used the Bender's decomposition and a convex ACOPF model to optimize the operation of the energy hubs. Results showed that the decentralized model performed better than other centralized operation models. A network of cooperative energy hubs was modeled by [28] with the objective to reduce operating costs. The energy hubs considered electrical, heating, and cooling loads as well as ice storage within the model. The authors modeled the problem by using a combination of mixed-integer linear programming and coalitional game theory to coordinate the energy hubs. The authors did not consider

demand response programs in the model. A centralized framework for solving the coordinated operation of energy hubs in the presence of industrial, commercial, and residential hubs has been proposed in [29] while the ACOPF problem was considered in a sequential and iterative sub-problem in the optimization problem. However, the main challenging issue in the distribution networks are the voltage drops [30] and congestion or overloading of the distribution feeders [31] and it must be considered in the embedded models during both normal and contingent conditions.

This section has reviewed and critically evaluated the existing literature. Several gaps in the literature were identified and in the next section, these gaps will be addressed through the contributions of the present paper.

C. Main Contributions

The optimality and feasibility issues should be addressed in the optimization problem to more precisely investigate the multi-hub operation in a distribution system. Accordingly, different types of energy hubs including industrial, commercial, and residential hubs, have been modeled and studied. The decentralized optimization model has been used to solve the OPF problem. In this regard, the OPF problem has been studied using both integrated and coordinated models. Moreover, the MILP framework has been employed to analyze the optimal operation problem of the energy hub. Accordingly, the main contributions of this paper compared to the existing literature are as follows:

1- Developing an energy trading mechanism between different hubs in the distribution network utilizing an ADMM based OPF (ADMM-OPF) model.

2- Addressing the P2P transactions for electrical energy trading between the grid participants.

3- Increasing the ability of power exchange between the energy hubs.

4- Presenting a MILP model for multi-carrier energy systems.

D. Paper Organization

This paper is organized as follows: The ADMM framework for solving the standard optimization problem is presented in Section 2. This decentralized framework addresses the data privacy of the clients while solving the optimization problem with the minimum data exchange. The mathematical problem formulation is introduced in Section 3, focusing on the application of the ADMM for the OPF application as well as a generalized optimization model for operating multi-carrier energy hubs. For the sake of simplicity, the energy hub operation problem is investigated in the MILP framework. The mathematical formulation of this problem is presented for two different market mechanisms. The first mechanism, named "integrated operation", relates to the grid-hub power transactions while in the second mechanism, called "coordinated operation", the P2P electrical energy trading is applicable with a certain pricing mechanism for all stakeholders. The simulation results for the different case studies are analyzed in Section 4, and the concluding remarks and future works are presented in the last section of this paper.

2- Decentralized Optimization Framework based on ADMM

The problem in a decentralized optimization framework, using the ADMM would be expressed as follows:

$$\underset{x,z}{Min} \quad f(x)+g(z) \tag{1a}$$

subject to:

$$Ax+Bz=c \tag{1b}$$

The objective should be minimized to determine the optimal values of the variables, x and z. The principle of this method is based on updating the decision variables as well as Lagrangian multipliers of the problem. The augmented Lagrangian relaxation can be represented as:

$$L_{\rho}(x,z,\lambda) := f(x)+g(z)+\lambda^{T}\left(Ax+Bz-c\right)+\frac{\rho}{2}\left\|Ax+Bz-c\right\|_{2}^{2} \tag{1c}$$

It is noteworthy that the Lagrangian multipliers of expression (1a) are denoted by λ^{k} and the positive parameter ρ is pre-determined, while $\left\|\bullet\right\|_{2}$ indicates the ℓ_{2}-norm of a vector. The ADMM uses an iterative process, where k shows the index of iterations of the ADMM. The decision variables would

be individually considered using the ADMM technique and the problem is tackled through several iterations to achieve the optimal solution with sufficient accuracy.

$$x^{k+1} := \arg\min_{x} L_{\rho}(x, z^{k}, \lambda^{k}) \tag{1d}$$

$$z^{k+1} := \arg\min_{z} L_{\rho}(x^{k+1}, z, \lambda^{k}) \tag{1e}$$

$$\lambda^{k+1} := \lambda^{k} + \rho\left(Ax^{k+1} + Bz^{k+1} - c\right) \tag{1f}$$

The primal residual of the balance constraint is as follow:

$$r^{k+1} := Ax^{k+1} + Bz^{k+1} - c \tag{1g}$$

The termination criterion for the iterative optimization problem according to the primal residual is as follows:

$$\left\|r^{k}\right\| \leq \varepsilon \tag{1h}$$

3. Problem Formulation

3.1. Decentralized ACOPF model

The general problem formulation for an ACOPF model is as follows. A two-bus test system for the OPF problem definition using the ADMM technique concept has been depicted in Fig. 1:

Min

$$\sum_{i=1}^{NG}\sum_{t=1}^{NT} f\left(PG_{i,t}\right) \tag{2a}$$

Subject to:

$$\underline{PG_i} \leq PG_{i,t} \leq \overline{PG_i} \qquad \forall i \in NG \tag{2b}$$

$$\underline{QG_i} \leq QG_{i,t} \leq \overline{QG_i} \qquad \forall i \in NG \tag{2c}$$

$$\underline{|V_i|^2} \leq |V_i|^2 \leq \overline{|V_i|^2} \qquad \forall i \in NB \tag{2d}$$

$$\underline{\Delta\theta_{ij}} \leq \theta_{i,t} - \theta_{j,t} \leq \overline{\Delta\theta_{ij}} \qquad \forall \{i, j\} \in NB \tag{2e}$$

$$PG_{i,t} - PD_{i,t} = PN_{i,t} \qquad \forall i \in NB \tag{2f}$$

$$QG_{i,t} - QD_{i,t} = QN_{i,t} \qquad \forall i \in NB \tag{2g}$$

$$PN_{i,t} + jQN_{i,t} = V_{i,t}\sum_{j\in B_i} Y^{*}_{i,j,t} V^{*}_{j,t} \qquad \forall i \in NB \tag{2h}$$

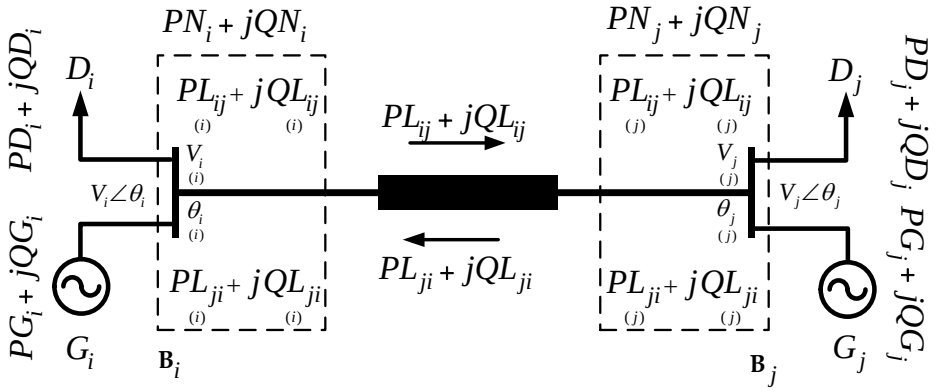

Fig. 1 A two-bus test system for the OPF problem definition using the ADMM technique concept.

The objective is to minimize the cost of serving electrical energy, while in this case, the energy cost is assumed to be a predefined tariff, i.e. time-of-use (TOU) tariff. The OPF constraints are stated in (2b)-(2h). Inequalities (2b) and (2c) show the limitations of the active and reactive power, respectively. The constraints (2d) and (2e) indicate the limitations of the bus voltage magnitude and voltage angle, respectively. Eqs. (2f) and (2g) relate to the net active and reactive power, respectively. Also, Eq. (2h) states the power injected into transmission lines.

The decentralized OPF problem using the ADMM approach can be written as follows:

$$x := \left\{ \left[PG_{i,t}, QG_{i,t} \right]_{i\in NG}, \left[PL_{ij,t}, QL_{ij,t}, V_{i,t}V_{j,t}, \theta_{ij,t} \right]_{\{i,j\}\in NL} \right\} \tag{3a}$$

$$z := \left\{ \left[\underset{(i)}{PG_{i,t}}, \underset{(i)}{QG_{i,t}} \right]_{i\in NG}, \left[\underset{(i)}{PL_{ij,t}}, \underset{(i)}{QL_{ij,t}} \right]_{\{i,j\}\in NL} \left[V_{i,t}^2, \theta_{i,t} \right]_{i\in NB} \right\} \tag{3b}$$

$$\lambda := \left\{ \left[\lambda_{i,t}^{PG}, \lambda_{i,t}^{QG} \right]_{i\in NG}, \left[\lambda_{ij,t}^{PL_{ij}}, \lambda_{ij,t}^{QL_{ij}}, \lambda_{ij,t}^{V_iV_j}, \lambda_{ij,t}^{\theta_{ij}} \right]_{\{i,j\}\in NL} \right\} \tag{3c}$$

According to the ADMM technique, the corresponding decision variables are addressed in (3a) and (3b). The dual variables, corresponding to the problem constraint, are addressed as a set of associated Lagrange multipliers in (3c). The ADMM technique is applied to update the generators decision variables:

$$x_{i,t}^{k+1,G} := \underset{x_{i,t}^{G}}{\arg\min} \left[\sum_{i=1}^{NG} \sum_{t=1}^{NT} f\left(PG_{i,t}\right) + \left\langle \lambda_{i,t}^{k,G} x_{i,t}^{k,G} \right\rangle + \frac{\rho}{2} \left(\left\| PG_{i,t} - \underset{(i)}{PG_{i,t}^{k}} \right\|_2^2 + \left\| QG_{i,t} - \underset{(i)}{QG_{i,t}^{k}} \right\|_2^2 \right) \right] \tag{3d}$$

where $x_{i,t}^{G} := \left[PG_{i,t}, QG_{i,t} \right]$ and $\lambda_{i,t}^{G} := \left[\lambda_{i,t}^{PG}, \lambda_{i,t}^{QG} \right]$.

For the given transmission lines, the corresponding decision variables can be stated as below:

$$x_{ij,t}^{k+1,L} := \arg\min_{x_{ij,t}^{L}} \left[\begin{array}{l} \left\langle \left[\lambda_{ij,t}^{k,L}, \lambda_{ji,t}^{k,L} \right], x_{ij,t}^{k,L} \right\rangle + \\ \sum_{(l,k)\in NL} \frac{\rho}{2} \left(\left\| \left(V_{l,t}^{k}\right)^2 - V_{l,t} V_{m,t} \right\|_2^2 + \left\| \theta_{l,t}^{k} - \theta_{lm,t} \right\|_2^2 + \left\| PL_{lm,t} - PL_{lm,t}^{k} \right\|_2^2 + \left\| QL_{lm,t} - QL_{lm,t}^{k} \right\|_2^2 \right) \end{array} \right] \quad (3e)$$

The local decision variables to be transferred to the other section can be written as:

$$z_{i,t}^{k+1} := \arg\min_{z_{i,t}} \left[\begin{array}{l} \sum_{i=1}^{NG} \sum_{t=1}^{NT} - \left(\left\langle \lambda_{i,t}^{k} \left[\underset{(i)}{PG_{i,t}^{k}}, \underset{(i)}{QG_{i,t}^{k}} \right] \right\rangle + \frac{\rho}{2} \left(\left\| PG_{i,t}^{k+1} - \underset{(i)}{PG_{i,t}} \right\|_2^2 + \left\| PG_{i,t}^{k+1} - \underset{(i)}{PG_{i,t}} \right\|_2^2 \right) \right) + \\ \sum_{j\in B_i} \sum_{t=1}^{NT} \left(- \left\langle \lambda_{ij,t}^{k} \left[\underset{(i)}{PL_{ij,t}}, \underset{(i)}{QL_{ij,t}}, V_{i,t}^2, \theta_{i,t} \right] \right\rangle + \frac{\rho}{2} \left(\left\| PL_{ij,t}^{k+1} - \underset{(i)}{PL_{ij,t}} \right\|_2^2 + \left\| QL_{ij,t}^{k+1} - \underset{(i)}{QL_{ij,t}} \right\|_2^2 \right) \right) \\ + \left\| V_{i,t}^2 - \left(V_{i,t}^{k+1}\right)^2 \right\|_2^2 + \left\| \theta_{i,t} - \theta_{i,t}^{k+1} \right\|_2^2 \end{array} \right] \quad (3f)$$

where $z_{i,t} := \left[\left(\underset{(i)}{PG_{i,t}^{k}}, \underset{(i)}{QG_{i,t}^{k}} \right), V_{i,t}^2, \theta_{i,t}, \left(\underset{(i)}{PL_{ij,t}^{k}}, \underset{(i)}{QL_{ij,t}^{k}} \right) \right]$ and $\lambda_{ij,t}^{k} := \lambda_{ij,t}^{V_i V_j}, \lambda_{ij,t}^{\theta_{ij}}$

3.2. Multi-Carrier Energy Hubs

For each peer in the MG, the minimization of the total cost is taken into consideration. The mathematical representation of the energy hub transactions is as follows, while the conceptual scheme of the studied hub is illustrated in Fig. 2.

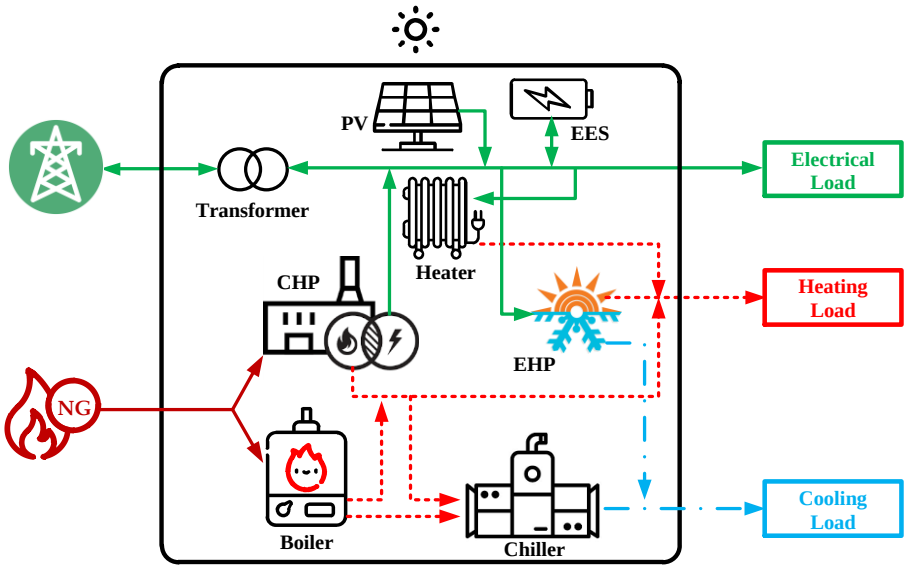

Fig. 2. The conceptual scheme of the studied hub [32].

Min

$$OF_k = \overbrace{\underbrace{\sum_{t=1}^{NT} f\left(CHP_{k,t}\right) + f\left(Boiler_{k,t}\right)}_{\text{Natural Gas Cost}} + \underbrace{\sum_{t=1}^{NT}\left[f\left(P_{k,t}^{G\to H}\right) - f\left(P_{k,t}^{H\to G}\right)\right]}_{\text{Centralized Transactions}}}^{\text{Integrated Operation}} + \underbrace{\sum_{m\neq k}\sum_{t=1}^{NT}\left[g\left(P_{k,t}^{P_m\to H}\right) - g\left(P_{k,t}^{H\to P_m}\right)\right]}_{\text{Peer-to-Peer Transactions}}}^{\text{Coordinated Operation}} \quad (4a)$$

$$f\left(CHP_{k,t}\right) = \left(\frac{P_{k,t}^{CHP}}{\eta_e^{CHP}} + \frac{H_{k,t}^{CHP}}{\eta_h^{CHP}}\right) NG_{k,t} \quad (4b)$$

$$f\left(Boiler_{k,t}\right) = \left(\frac{H_{k,t}^{Boiler}}{\eta_h^{Boiler}}\right) NG_{k,t} \quad (4c)$$

$$f\left(P_{k,t}^{G\to H}\right) = P_{k,t}^{G\to H}\pi_{k,t}^{G\to H} \quad (4d)$$

$$f\left(P_{k,t}^{H\to G}\right) = P_{k,t}^{H\to G}\pi_{k,t}^{H\to G} \quad (4e)$$

$$g\left(P_{k,t}^{P_m\to H}\right) = P_{k,t}^{P_m\to H}\pi_{k,t}^{P_m\to H} \quad m\neq k \quad (4f)$$

$$g\left(P_{k,t}^{H\to P_m}\right) = P_{k,t}^{H\to P_m}\pi_{k,t}^{H\to P_m} \quad m\neq k \quad (4g)$$

The objective function defined for each peer is to minimize the total cost, which is comprised of three items. The first item indicates the cost due to the NG procurement through the NG system. It is worth noting that the CHP unit and boilers use NG while an hourly tariff is applied to every sector, i.e. industrial, commercial and residential sectors. The costs due to the centralized and P2P power transactions with the utility grid and other peers are modeled in the second and third items, respectively. Each peer uses the market hourly prices. Accordingly, the system operator should execute a regulated market and bills will be calculated for the values collected by smart meters in each sector. The costs, imposed by employing the CHP and boiler, are shown by functions (4b) and (4c), respectively. Expressions (4d)-(4g) state the cost/income due to purchasing/selling electricity in the centralized and P2P modes. A convex feasible operating region (FOR) using binary variables, has been used to characterize the CHP operation as follows [33].

$$\underline{P_k^{CHP}} I_{k,t}^{CHP} \le P_{k,t}^{CHP} \le \overline{P_k^{CHP}} I_{k,t}^{CHP} \quad (5a)$$

$$\underline{H_k^{CHP}} I_{k,t}^{CHP} \le H_{k,t}^{CHP} \le \overline{H_k^{CHP}} I_{k,t}^{CHP} \quad (5b)$$

$$\underline{S_k^{CHP}} I_{k,t}^{CHP} \le P_{k,t}^{CHP} + H_{k,t}^{CHP} \le \overline{S_k^{CHP}} I_{k,t}^{CHP} \quad (5c)$$

$$P_{k,t}^{CHP} = P_{k,t}^{CHP\to G} + P_{k,t}^{CHP\to EL} + P_{k,t}^{CHP\to EH} + P_{k,t}^{CHP\to EES} + P_{k,t}^{CHP\to EHP} + \sum_{m\neq k} P_{k,t}^{CHP\to P_m} \quad (5d)$$

$$H_{k,t}^{CHP} = H_{k,t}^{CHP \to HL} + H_{k,t}^{CHP \to AC} \quad (5e)$$

Equations (5a)-(5c) deal with the lower and upper bounds of the electrical power generation, heat generation, and the total capacity of CHP units. The hourly binary variable, $I_{k,t}^{CHP}$, states that if the CHP unit is running, the power and heat generated should be within the limits of the unit. The power generated by the CHP unit can be delivered to the load, the utility grid, the electric heater (EH), the battery to charge, or it can be sold to other hubs. The heat generated is also delivered to heating load demands or the absorption chiller (AC).

The boiler should operate within the permitted operating interval (6a). The heat generated by the boiler follows the same behavior as that of the CHP system and it is stated in (6b).

$$\underline{H_k^{Boiler}} I_{k,t}^{Boiler} \le H_{k,t}^{Boiler} \le \overline{H_k^{Boiler}} I_{k,t}^{Boiler} \quad (6a)$$

$$H_{k,t}^{Boiler} = H_{k,t}^{Boiler \to HL} + H_{k,t}^{Boiler \to AC} \quad (6b)$$

The heat generated by the boiler is delivered to the heating load or AC.

Electric Heater Model:

Inequality (7a) states the operating limits of the electric heater. Relationship (7b) shows the heat generation equation of the EH indicated as the product of the input power and the system efficiency, denoted by $P_{k,t}^{EH}$ and η_h^{EH}, respectively [4]. It is also noteworthy that the CHP unit, the electrical energy storage (EES) system, the utility grid, or the power trading with other energy hubs would provide the power needed by the EH. Besides, the expression (7d) shows that the heat output of the EH would supply the heating load.

$$\underline{H_k^{EH}} I_{k,t}^{EH} \le H_{k,t}^{EH} \le \overline{H_k^{EH}} I_{k,t}^{EH} \quad (7a)$$

$$H_{k,t}^{EH} = P_{k,t}^{EH} \eta_h^{EH} \quad (7b)$$

$$P_{k,t}^{EH} = P_{k,t}^{G \to EH} + P_{k,t}^{CHP \to EH} + P_{k,t}^{EES \to EH} + \sum_{m \ne k} P_{k,t}^{P_m \to EH} \quad (7c)$$

$$H_{k,t}^{EH} = H_{k,t}^{EH \to HL} \quad (7d)$$

Electrical Heat Pump Model:

Inequalities (8a) and (8b) indicate that the heating power, $H_{k,t}^{EHP}$, and cooling power, $C_{k,t}^{EHP}$, produced by the electric heat pump (EHP) is constrained within the feasible operating interval, respectively. Furthermore, the operation modes of the EHP, i.e. heating and cooling operation modes, are determined by $I_{k,t}^{EHP,H}$ and $I_{k,t}^{EHP,C}$, respectively. It should be noted that the EHP is not capable of operating in the two modes, simultaneously as stated in (8c). Eqs. (8d) and (8e) show that the heating power and cooling power outputs of the EHP are the product of the input electrical power and the associated system efficiency, respectively. The electrical power balance equation is stated in Eq. (8f) while Eq. (8g) and Eq. (8h) indicate the heating and cooling power balance equations respectively.

$$\underline{H_k^{EHP}} I_{k,t}^{EHP,H} \le H_{k,t}^{EHP} \le \overline{H_k^{EHP}} I_{k,t}^{EHP,H} \tag{8a}$$

$$\underline{C_k^{EHP}} I_{k,t}^{EHP,C} \le C_{k,t}^{EHP} \le \overline{C_k^{EHP}} I_{k,t}^{EHP,C} \tag{8b}$$

$$0 \le I_{k,t}^{EHP,H} + I_{k,t}^{EHP,C} \le 1 \tag{8c}$$

$$H_{k,t}^{EHP} = P_{k,t}^{EHP} COP_h^{EHP} \tag{8d}$$

$$C_{k,t}^{EHP} = P_{k,t}^{EHP} COP_c^{EHP} \tag{8e}$$

$$P_{k,t}^{EHP} = P_{k,t}^{G\to EHP} + P_{k,t}^{CHP\to EHP} + P_{k,t}^{EES\to EHP} + \sum_{m\neq k} P_{k,t}^{P_m\to EHP} \tag{8f}$$

$$H_{k,t}^{EHP} = H_{k,t}^{EHP\to HL} \tag{8g}$$

$$C_{k,t}^{EHP} = C_{k,t}^{EHP\to CL} \tag{8h}$$

Absorption Chiller Model:

The absorption chiller (AC) should supply the cooling load demand by using the generation equation (9a) and its output is constrained as shown in inequality (9b). Eq. (9c) states that the power required by the AC would be provided by the CHP unit and the boiler. Besides, the cooling power flow of the AC is shown in expression (9d).

$$C_{k,t}^{AC} = H_{k,t}^{AC} \eta_c^{AC} \tag{9a}$$

$$\underline{C_k^{AC}} I_{k,t}^{AC} \le C_{k,t}^{AC} \le \overline{C_k^{AC}} I_{k,t}^{AC} \tag{9b}$$

$$H_{k,t}^{AC} = H_{k,t}^{CHP\to AC} + H_{k,t}^{Boiler\to AC} \tag{9c}$$

$$C_{k,t}^{AC} = C_{k,t}^{AC\to CL} \tag{9d}$$

Electrical Energy Storage Model:

The hourly energy balance equation of the EES system has been shown in Eq. (10a) while the upper and lower bounds of the energy stored in the system are applied through inequality (10b) [34]. The energy available at hour *t* depends upon the amount of energy available in the previous hour as well as the charging/discharging power at time *t* taking into consideration the system efficiency in each of the two modes. Furthermore, the charging and discharging rates are constrained as stated in (10c) and (10d), respectively. The binary variable, $I_{k,t}^{EES,Ch.}$, specifies the charging mode, while the discharging mode is specified by using the binary variable $I_{k,t}^{EES,Dis.}$. As constraint (10e) shows, the EES system can only operate in either discharging mode or charging mode at a given time [35]. To meet the operation requirements of the subsequent scheduling period, the energy that should be available at the final interval of the scheduling period must be equal to that of the initial time interval as indicated by constraint (10f), while the amount of energy available at the beginning of the scheduling period is determined by Eq. (10g). The energy flows in the charging and discharging modes are expressed in (10h) and (10i), respectively.

$$E_{k,t}^{EES} = E_{k,t-1}^{EES} + \left(P_{k,t}^{EES,Ch.}\eta_{k,Ch.}^{EES}\right) - \left(\frac{P_{k,t}^{EES,Dis.}}{\eta_{k,Dis.}^{EES}}\right) \tag{10a}$$

$$\underline{E_k^{EES}} \le E_{k,t}^{EES} \le \overline{E_k^{EES}} \tag{10b}$$

$$0 \le P_{k,t}^{EES,Ch.} \le \overline{P_k^{EES,Ch.}} I_{k,t}^{EES,Ch.} \tag{10c}$$

$$0 \le P_{k,t}^{EES,Dis.} \le \overline{P_k^{EES,Dis.}} I_{k,t}^{EES,Dis.} \tag{10d}$$

$$0 \le I_{k,t}^{EES,Ch.} + I_{k,t}^{EES,Dis.} \le 1 \tag{10e}$$

$$E_{k,t=NT}^{EES} = E_{k,t=0}^{EES} \tag{10f}$$

$$E_{k,t=0}^{EES} = \alpha_k \overline{E_k^{EES}} \tag{10g}$$

$$P_{k,t}^{EES,Ch.} = P_{k,t}^{G\to EES} + P_{k,t}^{CHP\to EES} + P_{k,t}^{PV\to EES} + \sum_{m\neq k} P_{k,t}^{P_m\to EES} \tag{10h}$$

$$P_{k,t}^{EES,Dis.} = P_{k,t}^{EES\to EL} + P_{k,t}^{EES\to G} + P_{k,t}^{EES\to EH} + P_{k,t}^{EES\to EHP} + \sum_{m\neq k} P_{k,t}^{EES\to P_m} \tag{10i}$$

PV Power Generation Model:

The hourly power generation of the PV system is dependent upon the solar irradiance, the temperature, and the characteristics of the panel. Equation (11a) presents the power generated by the PV panel [36], and the energy flow equation of the PV system is indicated by expression (11b). The parameters of the PV system generation are extracted from [36] while the same irradiance values have been considered in this study for each hub. It is evident that the PV power generation is equal or less than the rated capacity of the installed PV system. As this equation shows, the power produced by the PV panel can be consumed by the electrical load, the EHP, and the EH, or even sold to the utility grid or other peers.

$$P_{k,t}^{PV} = \frac{G_{k,t}^{a}}{G_{0}^{a}}\left[\overline{P_{k}^{PV}} + \mu_{\overline{P}}\left(T_{k,t}^{a} + G_{k,t}^{a}\frac{NOCT-20}{800} - T_{0}^{M}\right)\right] \tag{11a}$$

$$P_{k,t}^{PV} = P_{k,t}^{PV\to EL} + P_{k,t}^{PV\to G} + P_{k,t}^{PV\to EES} + P_{k,t}^{PV\to EHP} + P_{k,t}^{PV\to EH} + \sum_{m\neq k} P_{k,t}^{PV\to P_m} \tag{11b}$$

Power Transaction with the Distribution Network:

Equations (12a)-(12e) show the power transacted between the hub and the utility grid. The amount of power sold to the upstream system can be provided by the CHP unit, the EES system, or the PV panel as shown in (12a). Besides, the power purchased from the upstream system can be delivered to the EES system, the EH, the EHP, or directly consumed by the electrical loads. The maximum power that can be transacted between the energy hub and the utility grid is limited to the capacity of the transformer connecting these two systems as expressed in (12c) and (12d). It is noteworthy that the power transaction is a positive variable to specify the difference between the power purchased and sold from/to the grid. The simultaneous selling and purchasing of power are not allowed as shown by constraint (12e).

$$P_{k,t}^{H\to G} = P_{k,t}^{CHP\to G} + P_{k,t}^{EES\to G} + P_{k,t}^{PV\to G} \tag{12a}$$

$$P_{k,t}^{G\to H} = P_{k,t}^{G\to EES} + P_{k,t}^{G\to EH} + P_{k,t}^{G\to EHP} + P_{s,t}^{G\to EL} \tag{12b}$$

$$0 \le P_{k,t}^{H\to G} \le \overline{P^{Tr}} I_{k,t}^{H\to G} \tag{12c}$$

$$0 \le P_{k,t}^{G\to H} \le \overline{P^{Tr}} I_{k,t}^{G\to H} \quad (12d)$$

$$0 \le I_{k,t}^{H\to G} + I_{k,t}^{G\to H} \le 1 \quad (12e)$$

Balance Equations:

The most important constraint of the presented problem is the power balance equation, expressed by constraints (13a)-(13c). As constraint (13a) indicates, the electrical load demand of the consumer can be supplied by using the upstream system, the EES system, the PV panel, and the CHP unit. It should be noted that all these variables are of positive type. Likewise, the heating and cooling power balance equations are stated by (13b) and (13c), respectively. The heating load demand would be supplied by the CHP unit, the boiler, the EHP in the heating mode, and the EH. The cooling load demand is also supplied by using the AC, and the EHP in the cooling mode.

$$P_{k,t}^{G\to EL} + P_{k,t}^{ESS\to EL} + P_{k,t}^{PV\to EL} + P_{k,t}^{CHP\to EL} + \sum_{k\neq m} P_{k,t}^{P_m\to H} = P_{k,t}^{EL} \quad (13a)$$

$$H_{k,t}^{CHP\to HL} + H_{k,t}^{Boiler\to HL} + H_{k,t}^{EHP\to HL} + H_{k,t}^{EH\to HL} = H_{k,t}^{HL} \quad (13b)$$

$$C_{k,t}^{EHP\to CL} + C_{k,t}^{AC\to CL} = C_{k,t}^{CL} \quad (13c)$$

3.3. P2P Market Mechanism

Expressions (14a)-(14f) show the power transaction mechanism between the hubs. As (14a) shows, the net power delivered by the hub *k*, is determined by the surplus power generation of the PV panel, the EES system, and the CHP unit. The power, purchased from other generators can be consumed by the electrical load, the battery in the charging mode, the EHP, or the EH. Constraints (14a) and (14d) force the unidirectional power transaction between the peers.

The maximum power that can be transacted between two hubs is shown by these two constraints and constraint (14d) ensures the unidirectional power flow at each time interval. It is worth mentioning that it is not possible to simultaneously purchase power from the upstream grid and sell it to other hubs as stated in (14e). As the energy tariffs for the industrial, commercial, and residential sectors are different, it is not permitted to purchase power from the upstream grid at a lower price and sell it to

other peers at a higher price. However, according to the P2P energy transaction regulations, it is possible to purchase power over the off-peak hours and store it in the EES system and sell it over peak-load hours at higher prices.

$$P_{k,t}^{H\to P_m} = P_{k,t}^{PV\to P_m} + P_{k,t}^{EES\to P_m} + P_{k,t}^{CHP\to P_m} \qquad \forall m \neq k \qquad (14a)$$

$$P_{k,t}^{P_m\to H} = P_{k,t}^{P_m\to EL} + P_{k,t}^{P_m\to EES} + P_{k,t}^{P_m\to EHP} + P_{k,t}^{P_m\to EH} \qquad \forall m \neq k \qquad (14b)$$

$$0 \le P_{k,t}^{H\to P_m} \le \overline{P_{k,t}^{H\to P_m}} I_{k,t}^{H\to P_m} \qquad \forall m \neq k \qquad (14c)$$

$$0 \le P_{k,t}^{P_m\to H} \le \overline{P_{k,t}^{P_m\to H}} I_{k,t}^{P_m\to H} \qquad \forall m \neq k \qquad (14d)$$

$$0 \le I_{k,t}^{P_m\to H} + I_{k,t}^{H\to P_m} \le 1 \qquad \forall m \neq k \qquad (14e)$$

$$0 \le I_{k,t}^{G\to H} + I_{k,t}^{H\to P_m} \le 1 \qquad \forall m \neq k \qquad (14f)$$

3.4. P2P Implementation Model

Fig. 3 depicts the flow of data and energy within the energy hub. Both integrated and coordinated operation models have been illustrated in this figure. The main core of the proposed model consists of an energy trading center with the corresponding market manager. The market manager is the main responsible for handling the interactions within the local energy market as well as the centralized energy tradings. In this framework, the electrical energy can be traded in the local market between the clients and upstream grid, while the NG will be fed to the end-users and there is no way to buy the NG from the entities. In the integrated operation strategy, there is no possibility of trading energy between the peers while in the coordinated operation strategy, each peer has this opportunity to sell or buy electrical energy. The traded electrical energy will be transferred throughout the distribution company infrastructures and in this framework, the distribution system operator (DSO) is the responsible entity to address the energy losses as well as degradation cost of the infrastructures. The overall benefits of energy trading between the clients will cover the mentioned costs and it promotes the energy trading between the energy hubs within the local energy community.

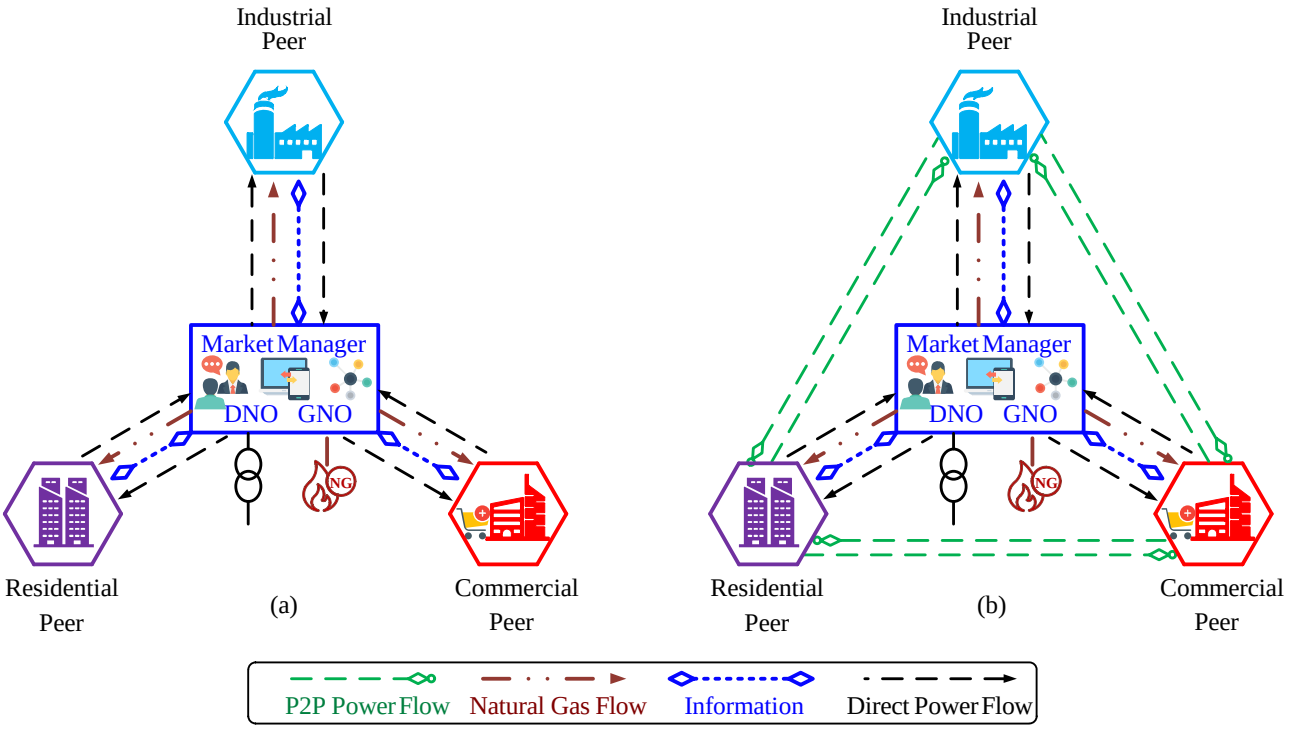

Fig. 3. Energy and data flow of the energy hub system, (a) integrated operation, (b) coordinated operation.

4- Simulation Results

The modified 33-bus distribution system has been used to simulate the problem and evaluate the developed framework. The system comprises of three energy hubs of industrial, commercial, and residential types connected to the system at nodes 23, 20, and 27, respectively. In the base case, i.e. without any heating and cooling load demands and without any local power generation, the optimal electrical energy flow has been investigated in the decentralized case by using both the ADMM technique as well as the centralized case. Then, the proposed model is utilized for both integrated operation and coordinated operation of the distribution network in the presence of energy hubs and their contributions in the daily operation are studied. Fig. 4 illustrates the integrated electricity and NG systems under consideration. Technical parameters of the hub assets are presented in Table 1.

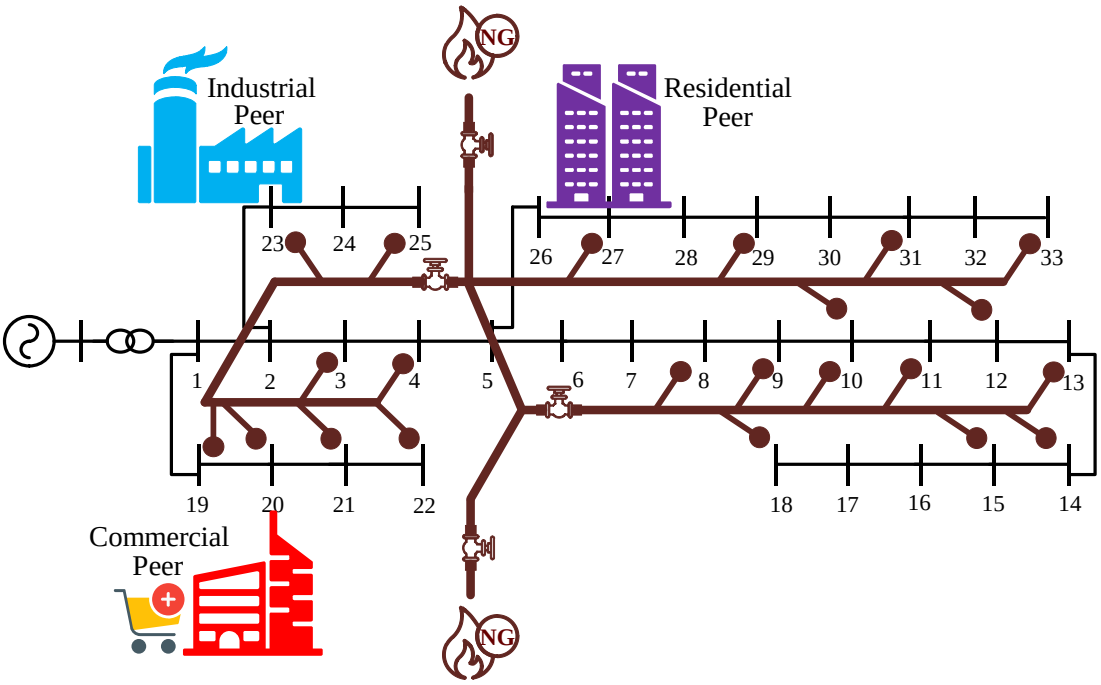

Fig. 4. The electric and NG systems used for the study.

Table 1. Technical parameters of hub assets.

Asset	Parameter	Unit	Industrial	Commercial	Residential
AC	$\overline{C_k^{AC}}$	kW	750	200	400
	$\underline{C_k^{AC}}$	kW	0	0	0
	η_c^{AC}	-	0.85	0.85	0.85
Boiler	$\overline{H_k^{Boiler}}$	kW	400	150	150
	$\underline{H_k^{Boiler}}$	kW	100	50	50
	η_h^{Boiler}	-	0.40	0.40	0.40
CHP	$\overline{S_k^{CHP}}$	kW	1400	1400	1400
	S_k^{CHP}	kW	200	200	200
	$\overline{P_k^{CHP}}$	kW	800	800	800
	$\underline{P_k^{CHP}}$	kW	0	0	0
	$\overline{H_k^{CHP}}$	kW	1000	1000	1000
	$\underline{H_k^{CHP}}$	kW	200	200	200
	η_e^{CHP}	-	0.45	0.45	0.45
	η_h^{CHP}	-	0.35	0.35	0.35
EES	$\overline{E_k^{EES}}$	kWh	600	300	300
	$\underline{E_k^{EES}}$	kWh	100	50	50
	$\overline{P_k^{EES,Ch.}}$	kW	50	25	25

	$\overline{P_k^{EES,Dis.}}$	kW	50	25	25
	α_k	-	0.333	0.333	0.333
	$\eta_{k,Ch.}^{EES}$	-	0.90	0.90	0.90
	$\eta_{k,Dis.}^{EES}$	-	0.90	0.90	0.90
EH	$\overline{H_k^{EH}}$	kW	300	100	100
	$\underline{H_k^{EH}}$	kW	0	0	0
	η_h^{EH}	-	0.85	0.90	0.90
EHP	$\overline{H_k^{EHP}}$	kW	200	150	300
	$\underline{H_k^{EHP}}$	kW	10	20	50
	$\overline{C_k^{EHP}}$	kW	200	150	300
	$\underline{C_k^{EHP}}$	kW	10	20	50
	COP_h^{EHP}	-	1.25	1.25	1.25
	COP_c^{EHP}	-	1.25	1.25	1.25
PV	$\overline{P_k^{PV}}$	kW	200	100	100

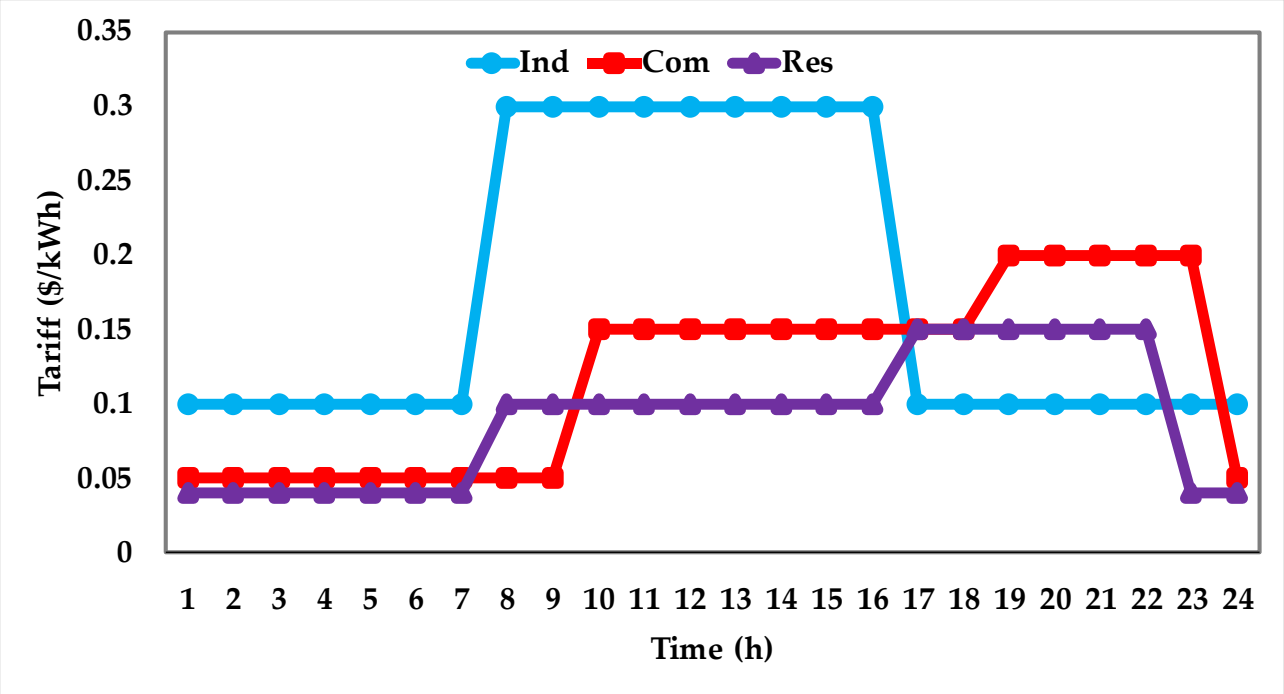

Fig. 5. The energy purchase price from the utility grid.

Fig. 5 represents the energy purchase tariffs. The tariffs for selling surplus energy for the industrial, commercial, and residential hubs are 70%, 80%, and 80% of the energy purchase tariff. Fig. 6

demonstrates the active load demand of the energy hubs. The power factor of the industrial, commercial, and residential loads are considered to be 0.8, 0.85, and 0.85, respectively which are constant over the scheduling period.

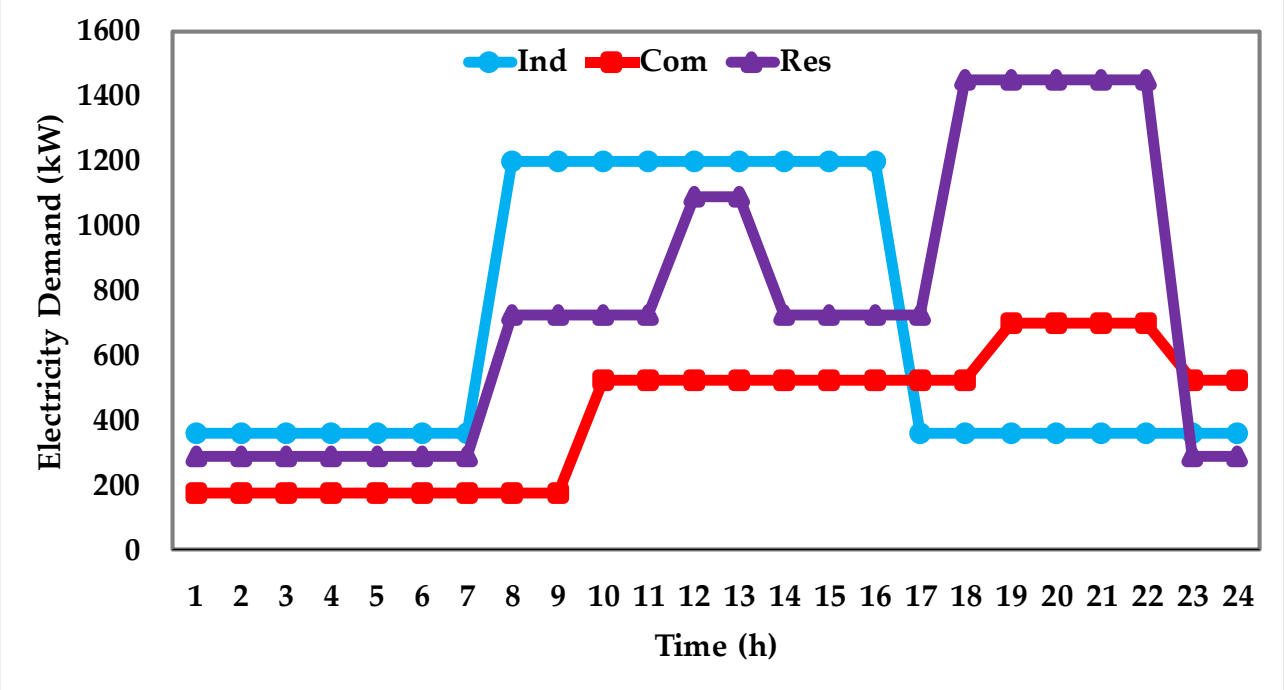

Fig. 6. The hourly active power demand of the studied energy hubs in the integrated operation mode.

4.1 Base Case Operation Results

To show the functionality of the proposed model, the application of ADMM in solving the optimal power flow is examined in this section. In the base case, the daily operation of the distribution network is studied while there is no power injection from the energy hubs. In other words, the distribution system feeds the total loads in the network. Therefore, comparing the results for the base case can be made through the classic power flow models. In this case, the voltage at the injection bus is fixed at 1.0 p.u.

The optimal power flow results are the same in the two cases as the distribution system can adequately supply the load demand. Accordingly, it can be concluded that the ACOPF results derived using the ADMM technique are valid and reliable. Table 2 provides the nodal active and reactive power

consumption. It can be seen that the total power consumption at the peak hour is 19.8737 MW+j12.0654MVAr. The industrial, commercial, and residential loads are 360 MW+j200 MVAr, 525 MW+j233.33 MVAr, and 1450 MW+j604.17 MVAr, respectively. It is noted that the power consumption of the commercial load at this hour is substantial and the industrial load consumes the baseload according to Fig. 6.

Table 2. Active and reactive power demand at peak hour (18:00h)

Bus	P (kW)	Q (kVAr)	Node	P (kW)	Q (kVAr)
Node 02	504.71	302.83	**Node 18**	454.24	201.88
Node 03	454.24	201.88	**Node 19**	454.24	201.88
Node 04	605.65	403.77	**Node 20**	525.00	233.33
Node 05	302.83	151.41	**Node 21**	454.24	201.88
Node 06	302.83	100.94	**Node 22**	454.24	201.88
Node 07	1009.42	504.71	**Node 23**	360.00	200.00
Node 08	1009.42	504.71	**Node 24**	2119.78	1009.42
Node 09	302.83	100.94	**Node 25**	2119.78	1009.42
Node 10	302.83	100.94	**Node 26**	302.83	126.18
Node 11	227.12	151.41	**Node 27**	1450.00	604.17
Node 12	302.83	176.65	**Node 28**	302.83	100.94
Node 13	302.83	176.65	**Node 29**	605.65	353.30
Node 14	605.65	403.77	**Node 30**	1009.42	3028.26
Node 15	302.83	50.47	**Node 31**	757.07	353.30
Node 16	302.83	100.94	**Node 32**	1059.89	504.71
Node 17	302.83	100.94	**Node 33**	302.83	201.88

The power flow results for the base case at the peak hour is presented in Table 3. In this table, the first and second columns are the sending and receiving ends, columns 3 and 4 are the sending ends' active and reactive power, while columns 5 and 6 provide the active and reactive power at the receiving ends. The feeders' active and reactive power losses are provided in the last two columns. The simulations results in both centralized and decentralized operation using ADMM are identical. It is noted that the centralized operation is performed by MATPOWER. The total amount of power losses at this hour is 1571.3761 kW+1057.3551kVAr.

Table 3. Power transmitted through the feeders at the peak hour (18:00h)

i	*j*	P_{ij}(MW)	Q_{ij}(MVAr)	P_{ji}(MW)	Q_{ji}(MVAr)	Ploss(kW)	Qloss(kVAr)
Node 01	**Node 02**	21.4451	13.1228	-21.3549	-13.0761	90.1538	46.6414
Node 02	**Node 03**	18.9546	11.9269	-18.5690	-11.7305	385.5812	196.3883
Node 03	**Node 04**	13.4542	9.2637	-13.2959	-9.1831	158.3316	80.6366
Node 04	**Node 05**	12.6902	8.7793	-12.5399	-8.7027	150.3472	76.5741
Node 05	**Node 06**	12.237	8.5513	-11.9280	-8.2845	309.0744	266.8078
Node 06	**Node 07**	5.6122	2.7439	-5.5992	-2.7007	13.0721	43.2106
Node 07	**Node 08**	4.5897	2.1960	-4.5097	-2.1382	80.0581	57.7772
Node 08	**Node 09**	3.5003	1.6335	-3.4714	-1.6128	28.8606	20.7348
Node 09	**Node 10**	3.1686	1.5118	-3.144	-1.4944	24.6086	17.4429
Node 10	**Node 11**	2.8411	1.3934	-2.8373	-1.3922	3.8295	1.2661
Node 11	**Node 12**	2.6102	1.2408	-2.6041	-1.2387	6.0985	2.0165
Node 12	**Node 13**	2.3013	1.0621	-2.2828	-1.0476	18.4716	14.5332
Node 13	**Node 14**	1.9800	0.8709	-1.9749	-0.8643	5.0543	6.6529
Node 14	**Node 15**	1.3693	0.4605	-1.3668	-0.4583	2.4768	2.2044
Node 15	**Node 16**	1.0640	0.4078	-1.062	-0.4064	1.9540	1.4269
Node 16	**Node 17**	0.7592	0.3054	-0.7574	-0.3031	1.7479	2.3336
Node 17	**Node 18**	0.4546	0.2022	-0.4542	-0.2019	0.3692	0.2895
Node 02	**Node 19**	1.8956	0.8464	-1.8945	-0.8454	1.1022	1.0518
Node 19	**Node 20**	1.4402	0.6435	-1.4344	-0.6382	5.8451	5.2669
Node 20	**Node 21**	0.9094	0.4049	-0.9088	-0.4041	0.6397	0.7474
Node 21	**Node 22**	0.4545	0.2023	-0.4542	-0.2019	0.2771	0.3664
Node 03	**Node 23**	4.6606	2.2649	-4.6410	-2.2515	19.6417	13.4210
Node 23	**Node 24**	4.2810	2.0515	-4.2479	-2.0253	33.1087	26.1440
Node 24	**Node 25**	2.1281	1.0159	-2.1198	-1.0094	8.2949	6.4905
Node 06	**Node 26**	6.0129	5.4397	-5.9890	-5.4275	23.8804	12.1637
Node 26	**Node 27**	5.6862	5.3013	-5.6553	-5.2856	30.9303	15.7481
Node 27	**Node 28**	4.2053	4.6814	-4.1291	-4.6143	76.1696	67.1573
Node 28	**Node 29**	3.8263	4.5133	-3.7734	-4.4673	52.8184	46.0141
Node 29	**Node 30**	3.1678	4.114	-3.1415	-4.1006	26.2788	13.3853
Node 30	**Node 31**	2.1321	1.0724	-2.1213	-1.0617	10.7697	10.6437
Node 31	**Node 32**	1.3642	0.7084	-1.3628	-0.7067	1.4411	1.6797
Node 32	**Node 33**	0.3029	0.2020	-0.3028	-0.2019	0.0890	0.1384

It is should be noted that the simulation time step is supposed to be 1 hour in this study and the loads are supposed to be constant at each hour. The amount of daily energy losses is 24144.4362 kWh+j16239.5971kVArh. Table 4 provides the hourly active and reactive power, and energy losses in the base case scenario. The voltage profile of the base scenario is depicted in the next section.

Table 4. The daily active and reactive losses in the base scenario

Hour	Ploss(kW)	Qloss(kVAr)	Hour	Ploss(kW)	Qloss(kVAr)
T01	523.5026	353.9953	**T13**	1247.0473	834.1745
T02	479.6929	324.2182	**T14**	1238.7669	831.5321
T03	454.6957	307.2324	**T15**	1314.0399	882.5659
T04	438.6580	296.3366	**T16**	1423.2936	956.6733
T05	471.7179	318.7987	**T17**	1453.0826	983.6319
T06	541.9198	366.5162	**T18**	1571.3761	1057.3551
T07	667.3331	451.8185	**T19**	1540.0185	1036.2450
T08	985.2178	659.5816	**T20**	1408.8562	947.2502
T09	1119.1774	750.2810	**T21**	1255.5290	843.2869
T10	1223.8077	821.3925	**T22**	1043.8493	699.9003
T11	1267.8470	851.2454	**T23**	671.5076	454.8767
T12	1276.2115	853.9063	**T24**	527.2878	356.7825

4.2 Integrated and Coordinated Operation Results

In this section, two scenarios were investigated for the optimal operation of the industrial, commercial, and residential hubs by utilizing the ADMM approach. In the first scenario, namely 'integrated operation', the operation of each hub's assets was studied separately and only power transaction with the upstream grid is allowed and this takes place at the connection nodes of the hubs. The results obtained from simulating the integrated scenario to supply the electrical, heating, and cooling load demands of each hub show that the local energy resources of each hub would be adequate to thoroughly supply the demand. Accordingly, the daily operating costs of the industrial, commercial, and residential hubs in the integrated scenario are \$3441.895, \$596.600, and \$988.789 respectively. The total operating cost of the hubs would be \$5027.284. In the coordinated scenario with the possibility of P2P energy transactions, the daily operating costs of the industrial, commercial, and residential hubs are \$2932.645, \$590.155, and \$914.165 respectively. The total operating cost of the energy hubs would be \$4436.965, which is lower than the integrated scenario by 11.75%. The largest decrease occurs in the industrial hub with 14.8% reduction while the smallest decrease occurs in the residential hub where costs are reduced by 1%. The industrial hub can make the largest profit by purchasing the surplus power generation from the commercial and residential hubs during hours 1-16 and at hour 24, and also by selling its surplus power generation to the other two hubs during

hours 17-23 in the coordinated scenario. Fig. 7 depicts the power transactions between the three hubs in the coordinated scenario.

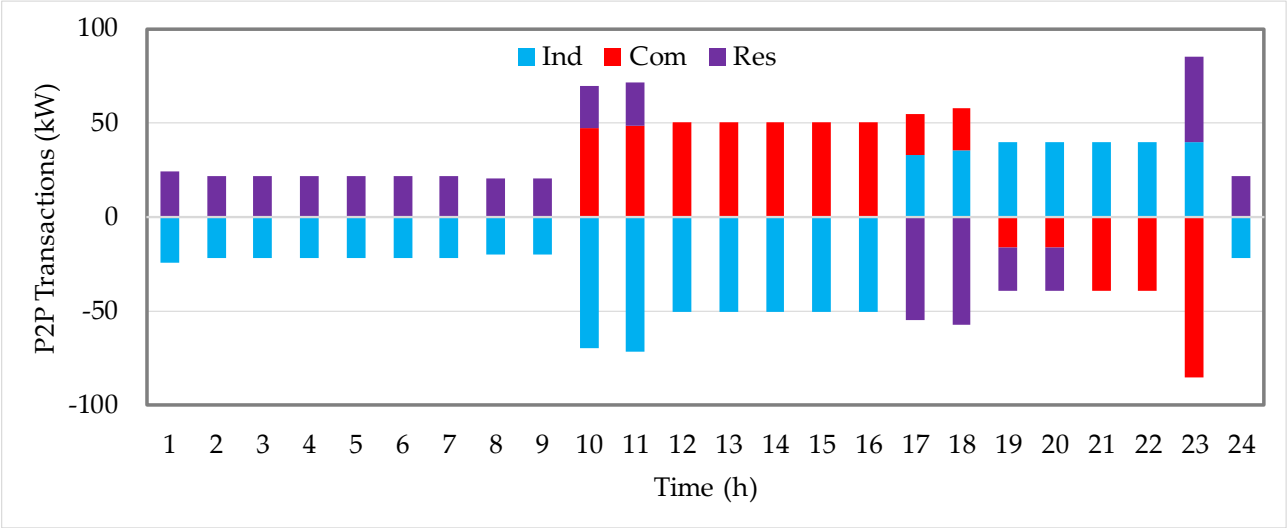

Fig. 7. Power transactions between the three hubs in the coordinated scenario.

The energy stored in the EES systems of the three hubs in the integrated and coordinated scenarios is shown in Fig. 8. Figs. 9-11 illustrate the power flow results, obtained by using the ADMM technique in the base case, the integrated scenario, and the coordinated scenario, respectively. In the base case, it is assumed that the hubs cannot actively participate in the market and thus transact power; so they are pure consumers. In this respect, the active power demands in the three cases are shown in Fig. 9. It is also noteworthy that the load demands of the industrial, commercial, and residential hubs are substantial. As a result, the local power generation in the hubs not only reduces the operating costs but also mitigates the total energy losses of the distribution system and improves the voltage profile. The net energy purchased from the utility grid in the integrated scenario has considerably decreased as hubs can locally generate power to supply their load demands, independently. Consequently, the amount of energy, purchased from the utility grid has dramatically reduced. The decrease in the power required in the coordinated model is considerably lower than that of the integrated model.

The reductions in the load demand over the peak hour, i.e. hour 18, are 1.76 MW and 2.489 MW in the integrated and coordinated models, respectively. The highest reductions in the load demand in the integrated and coordinated modes are 2.458 MW and 2.792 MW, respectively. The lowest reduction occurs during hours 2-7 by 0.24 MW and 0.7 MW in the integrated and coordinated modes, respectively. As expected, the coordinated model is more effective than the integrated model in mitigating the dependency on the upstream electrical grid.

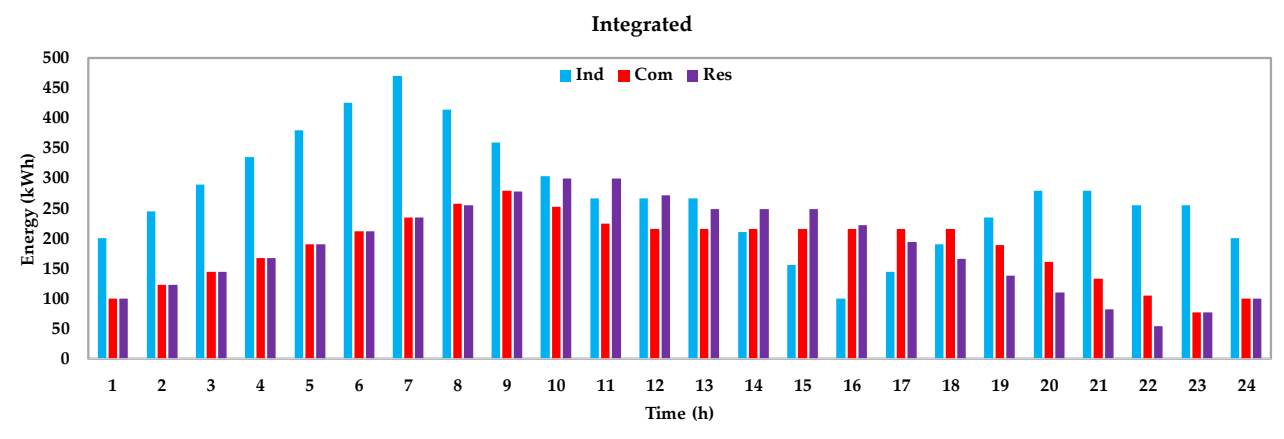

(a)

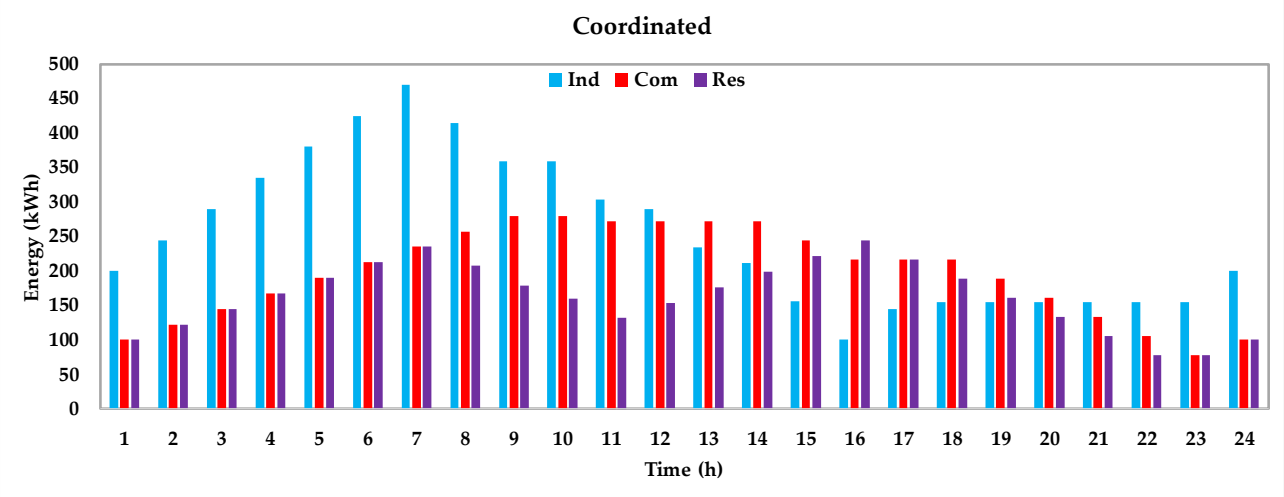

(b)

Fig. 8. The energy stored in the EES system of the three hubs, (a): integrated operation, (b): coordinated operation

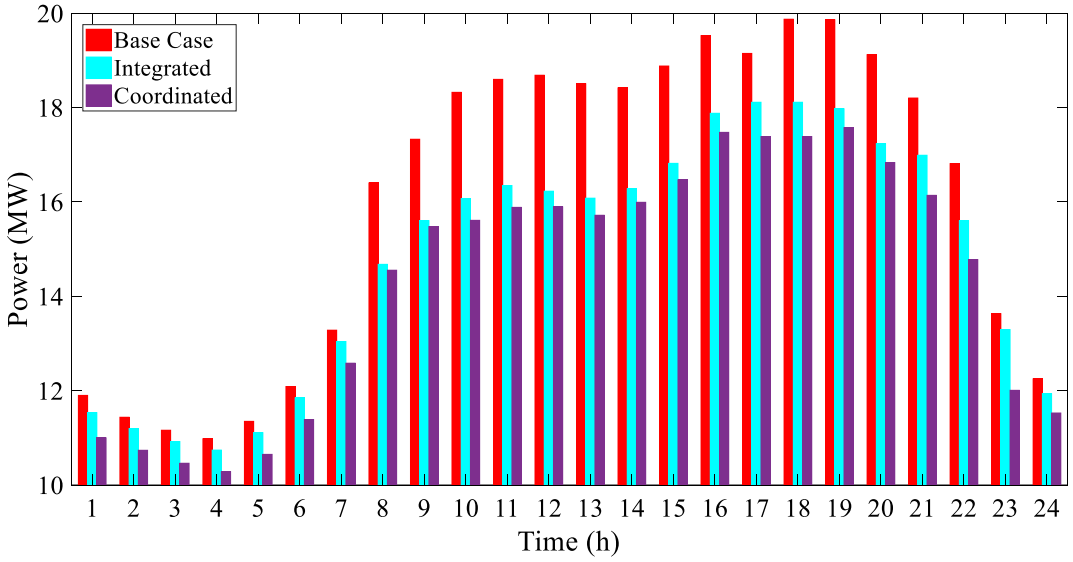

Fig. 9. The hourly active power demands of the distribution network for the base case, integrated case, and coordinated case.

The total power losses of the distribution system in the three operation cases are shown in Fig. 10. As can be observed, the losses are lower in the coordinated and integrated cases and as it is expected, the amount of power losses has been considerably reduced by using the local power generation in energy hubs. The voltage profiles of the industrial, commercial, and residential hubs are shown in Fig. 11. As this figure depicts, the voltage profiles of industrial, commercial, and residential loads are proportional to the peak load demand on that bus and the total load demand of the system. For instance, as Fig. 11(a) indicates the voltage profile significantly dropped during hours 8-16 at which the industrial peak load demand occurs. This trend in the subsequent hours is due to the indirect load demand increase of the commercial and residential energy hubs impacting the voltage profile of the industrial hub. As Fig. 11(b) illustrates, the highest voltage drop occurs at hour 19 with the load demand increase at this hour. However, the voltage profile has been enhanced through injecting power by the industrial hub in the coordinated and integrated models. It is noteworthy that batteries should charge to meet the constraint on the final state-of-charge (SoC) which in turn leads to the voltage drop during hours 20-21. Also, the voltage drop can be observed in

the residential hub during hours 17-22 due to the increase in the load demand. The voltage profile is improved over the final hours of the day with the decrease in the load demand.

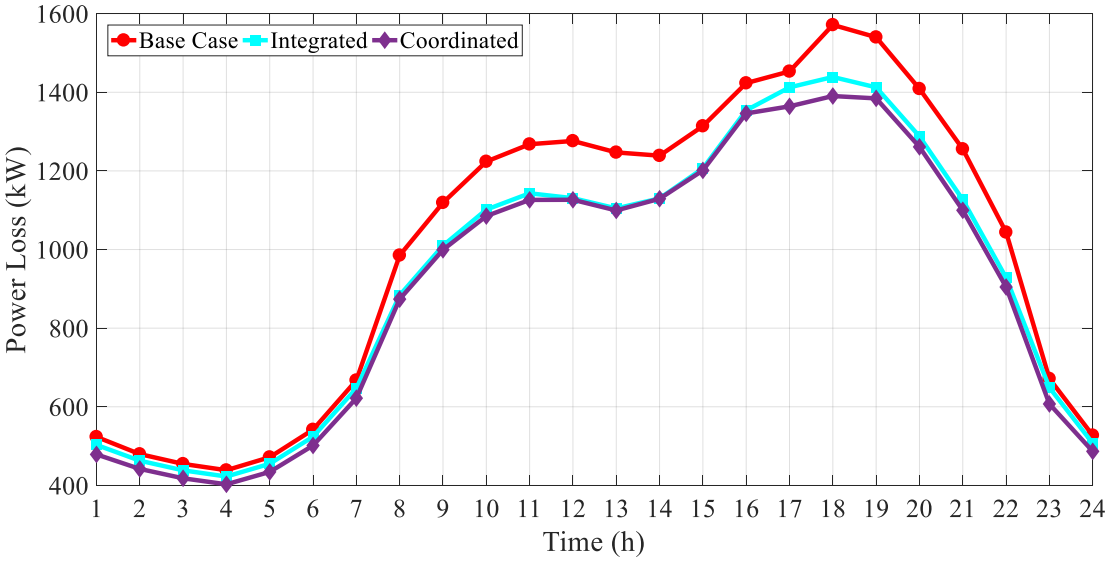

Fig. 10. The total hourly losses in the three operation cases.

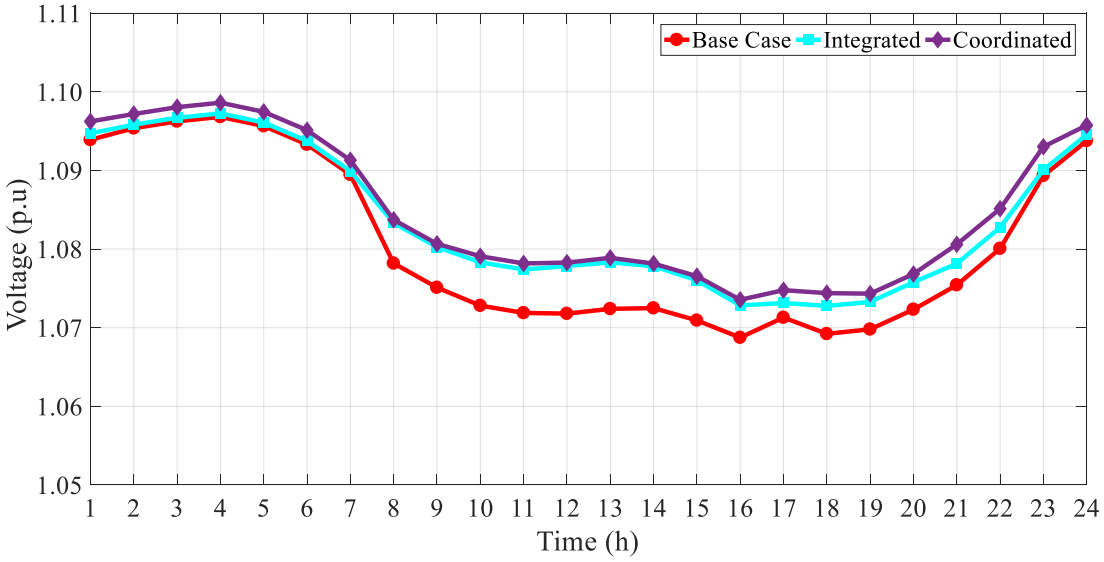

(a)

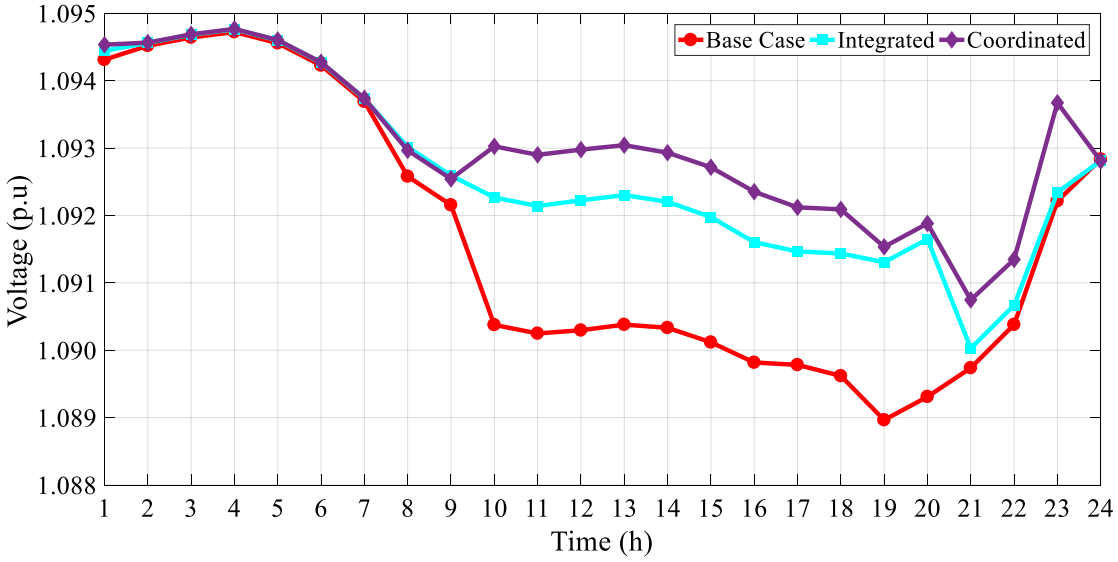

(b)

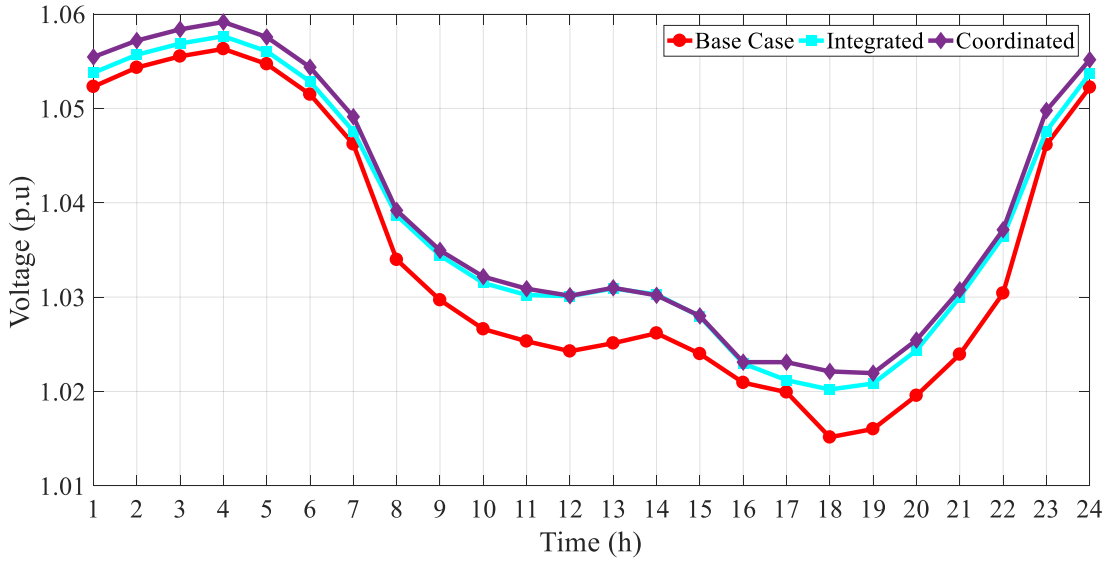

(c)

Fig. 11. Voltage profile of the industrial (a), commercial (b) and residential bus (c).

The power flow results derived by using the ADMM technique at hour 18, i.e. the peak hour, are illustrated in Figs. 12 and 13. The net values of power injected to the utility grid by the industrial, commercial, and residential hubs at this hour are 300.1444 kW, 184.4375 kW, and -205.693 kW at nodes 23, 20, and 27, respectively. Accordingly, the industrial and commercial hubs act as energy sellers and the residential hub is the buyer. Also, the power transaction between hubs is done as shown in Fig. 3. The residential hub has purchased 57.6375 kWh at hour 18 from the industrial and

commercial hubs, out of which 35.7 kWh has been provided by the industrial hub and 21.9375 kWh has been supplied by the commercial hub. Figs. 12 and 13 also show the power mismatch to better represent the convergence rate of the operation problem at hour 18. It is noted that the solution has converged after 98 iterations.

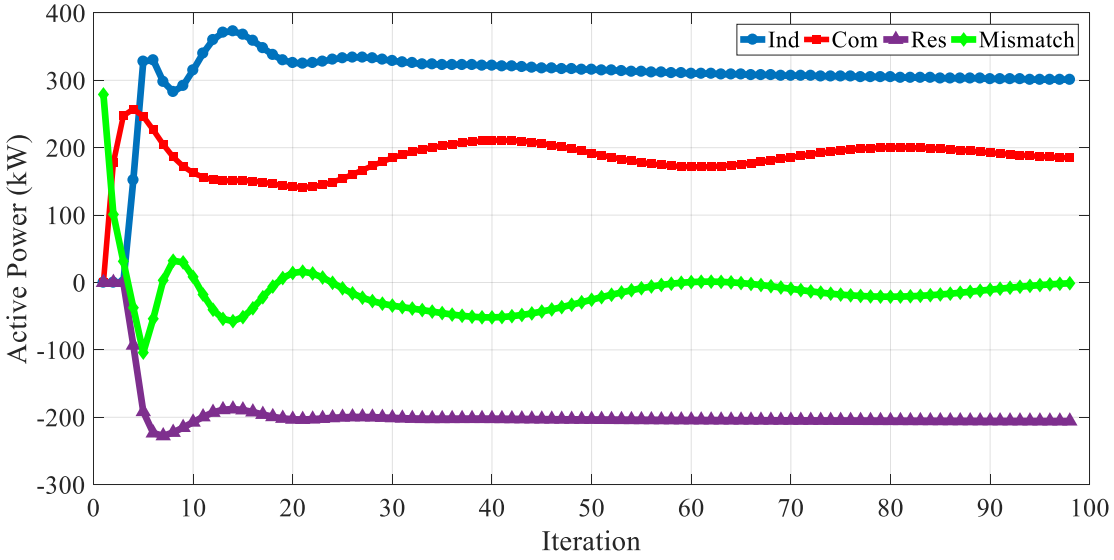

Fig. 12. The net active power of the studied hubs by using the ADMM technique.

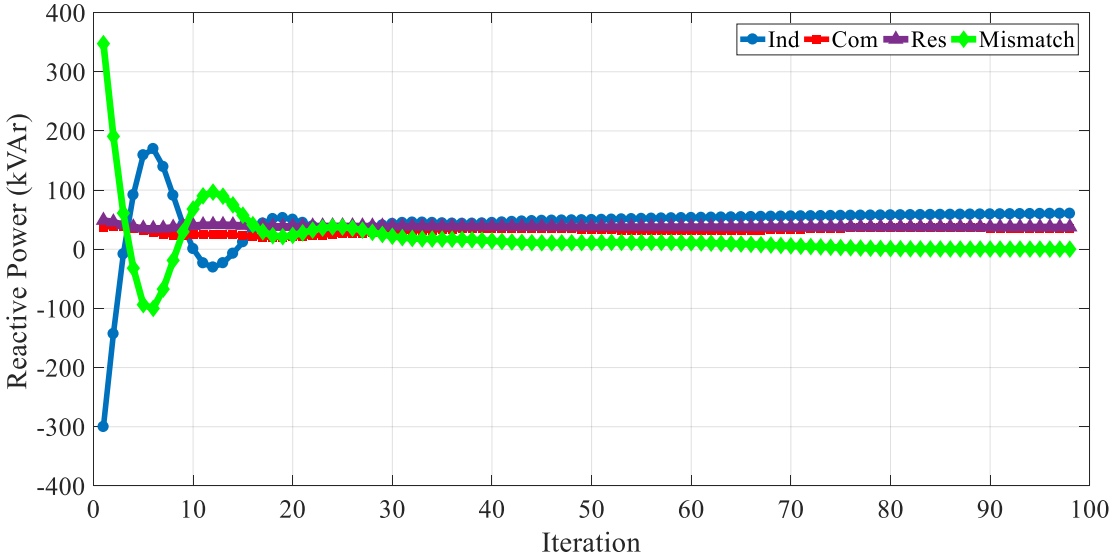

Fig. 13. The net reactive power of the studied hubs by using the ADMM technique.

Table 5 represents the operating costs of the three hubs and the total operating cost in the integrated and coordinated operation scenarios.

Table 5. Comparative results of the operation of the three energy hubs.

Hub	Integrated	Coordinated
Industrial ($)	3441.895	2932.645
Commercial ($)	596.600	590.155
Residential ($)	988.789	914.165
Total Cost ($)	5027.284	4436.965

5-Conclusion

This paper investigated the problem of the operation of energy hubs, including industrial, commercial, and residential hubs. In this respect, the hubs' assets were characterized using linear models. Besides, the operation problem of the hubs was investigated using different case studies. By employing the integrated model, the hub was only allowed to transact power with the utility grid based on a pre-determined tariff, which included the tax and grid cost. The coordinated operation model allowed the hubs to transact power with other hubs using the P2P energy trading mechanisms. As a result, the priority of the hubs would be to trade energy through P2P transactions rather than transacting power with the utility grid. In addition to effectively addressing the data privacy issue of clients and hub operators, the ADMM-OPF implemented in this paper ensures the minimum data exchange between the clients. The results obtained from simulating the problem for a typical day on an hourly basis verified that the coordinated operation model could substantially reduce the consumers' costs compared to the integrated operation model. Moreover, the energy losses were significantly reduced in comparison with both the base case and the integrated operation model, while the voltage profile of the system was considerably improved. As the presented model was based on the energy hubs participation in the P2P energy trading framework, future research would be conducted on the following items:

- Providing the capability of making bilateral contracts with price agreement and two degrees of freedom, i.e. the amount of power and the price.

- Extending the proposed model using the model predictive control in the presence of renewable energies, such as wind power generation, and modifying the energy trading strategy to include the intraday market.

The results, derived from simulating the presented modes showed that the coordinated model is more effective in reducing the total costs where the reduction in the costs was 11.75% more than the integrated scenario. For instance, the total costs reported for the industrial energy hub in the integrated and coordinated models were $3441.895 and $2932.645, respectively showing that by using the coordinated model, this cost could reduce by $509.25. The total costs of the commercial and residential hubs in the coordinated model with respect to the integrated model were mitigated by $6.450 and $74.524, respectively. It was observed that employing the coordinated model led to 17% drop in the total load demand while the integrated model resulted in 13% drop in the total load demand. In this regard, the industrial hub's load demand reduced by 14.8% which was the largest rate among the three hubs. On the other hand, the residential hub's load demand reduced by 1% which was the smallest rate compared to other hubs. The obtained results also depicted that it is possible for the industrial hub to make the largest profit by purchasing the surplus power generation from the commercial and residential hubs during hours 1-16 and at hour 24, and also by selling its surplus power generation to the other two hubs during hours 17-23 in the coordinated scenario.

Acknowledgment

J.P.S. Catalão and M.S. Javadi acknowledge the support by FEDER funds through COMPETE 2020 and by Portuguese funds through FCT, under POCI-01-0145-FEDER-029803 (02/SAICT/2017).

References

[1] Mansourlakouraj M, Sanjari MJ, Javadi MS, Shahabi M, Catalao JPSPS. Exploitation of Microgrid Flexibility in Distribution System Hosting Prosumers. IEEE Trans Ind Appl 2021:1–1. https://doi.org/10.1109/TIA.2021.3073882.

[2] Li H, Rezvani A, Hu J, Ohshima K. Optimal day-ahead scheduling of microgrid with hybrid

electric vehicles using MSFLA algorithm considering control strategies. Sustain Cities Soc 2021;66:102681. https://doi.org/10.1016/j.scs.2020.102681.

[3] Javadi M, Nezhad AE, Gough M, Lotfi M, Catalao JPS. Implementation of Consensus-ADMM Approach for Fast DC-OPF Studies. 2019 Int. Conf. Smart Energy Syst. Technol., IEEE; 2019, p. 1–5. https://doi.org/10.1109/SEST.2019.8848992.

[4] Javadi MS, Anvari-Moghaddam A, Guerrero JM. Robust energy hub management using information gap decision theory. Proc. IECON 2017 - 43rd Annu. Conf. IEEE Ind. Electron. Soc., vol. 2017- Janua, 2017. https://doi.org/10.1109/IECON.2017.8216073.

[5] Mansouri SA, Ahmarinejad A, Ansarian M, Javadi MS, Catalao JPS. Stochastic planning and operation of energy hubs considering demand response programs using Benders decomposition approach. Int J Electr Power Energy Syst 2020;120:106030. https://doi.org/10.1016/j.ijepes.2020.106030.

[6] Wasilewski J. Integrated modeling of microgrid for steady-state analysis using modified concept of multi-carrier energy hub. Int J Electr Power Energy Syst 2015;73:891–8. https://doi.org/10.1016/j.ijepes.2015.06.022.

[7] Shekari T, Gholami A, Aminifar F. Optimal energy management in multi-carrier microgrids: an MILP approach. J Mod Power Syst Clean Energy 2019;7:876–86. https://doi.org/10.1007/s40565-019-0509-6.

[8] Jordehi AR, Javadi MS, Shafie-khah M, Catalão JPS. Information gap decision theory (IGDT)-based robust scheduling of combined cooling, heat and power energy hubs. Energy 2021;231:120918. https://doi.org/10.1016/j.energy.2021.120918.

[9] Fotuhi-Firuzabad M. Day-ahead energy management framework for a networked gas–heat–electricity microgrid. IET Gener Transm Distrib 2019;13:4617-4629(12).

[10] Jordehi AR, Javadi MS, Catalão JPS. Day-ahead scheduling of energy hubs with parking lots for electric vehicles considering uncertainties. Energy 2021;229:120709. https://doi.org/10.1016/j.energy.2021.120709.

[11] Xu D, Zhou B, Chan KW, Li C, Wu Q, Chen B, et al. Distributed multienergy coordination of multimicrogrids with biogas-solar-wind renewables. IEEE Trans Ind Informatics 2019;15:3254–66. https://doi.org/10.1109/TII.2018.2877143.

[12] Wu G, Xiang Y, Liu J, Gou J, Shen X, Huang Y, et al. Decentralized day-ahead scheduling of multi-area integrated electricity and natural gas systems considering reserve optimization. Energy 2020;198:117271. https://doi.org/10.1016/j.energy.2020.117271.

[13] Zhao P, Gu C, Huo D, Shen Y, Hernando-Gil I. Two-Stage Distributionally Robust Optimization for Energy Hub Systems. IEEE Trans Ind Informatics 2020;16:3460–9. https://doi.org/10.1109/TII.2019.2938444.

[14] Qian T, Tang W, Wu Q. A fully decentralized dual consensus method for carbon trading power dispatch with wind power. Energy 2020;203:117634. https://doi.org/10.1016/j.energy.2020.117634.

[15] Yang L, Luo J, Xu Y, Zhang Z, Dong Z. A Distributed dual consensus admm based on partition for dc-dopf with carbon emission trading. IEEE Trans Ind Informatics 2020;16:1858–72. https://doi.org/10.1109/TII.2019.2937513.

[16] Ou M, Xue Y, Zhang XP. Iterative DC Optimal Power Flow Considering Transmission

Network Loss. Electr Power Components Syst 2016;44:955–65. https://doi.org/10.1080/15325008.2016.1147104.

[17] Kim J, Dvorkin Y. A P2P-dominant Distribution System Architecture. IEEE Trans Power Syst 2019:1–1. https://doi.org/10.1109/tpwrs.2019.2961330.

[18] Sorin E, Bobo L, Pinson P. Consensus-Based Approach to Peer-to-Peer Electricity Markets with Product Differentiation. IEEE Trans Power Syst 2019;34:994–1004. https://doi.org/10.1109/TPWRS.2018.2872880.

[19] Khorasany M, Mishra Y, Ledwich G. A Decentralized Bilateral Energy Trading System for Peer-to-Peer Electricity Markets. IEEE Trans Ind Electron 2020;67:4646–57. https://doi.org/10.1109/TIE.2019.2931229.

[20] Zia MF, Benbouzid M, Elbouchikhi E, Muyeen SM, Techato K, Guerrero JM. Microgrid Transactive Energy: Review, Architectures, Distributed Ledger Technologies, and Market Analysis. IEEE Access 2020;8:19410–32. https://doi.org/10.1109/access.2020.2968402.

[21] Abrishambaf O, Lezama F, Faria P, Vale Z. Towards transactive energy systems: An analysis on current trends. Energy Strateg Rev 2019;26:100418. https://doi.org/10.1016/j.esr.2019.100418.

[22] Wang X, Liu Y, Liu C, Liu J. Coordinating energy management for multiple energy hubs: From a transaction perspective. Int J Electr Power Energy Syst 2020;121:106060. https://doi.org/10.1016/j.ijepes.2020.106060.

[23] Nikmehr N. Distributed robust operational optimization of networked microgrids embedded interconnected energy hubs. Energy 2020;199. https://doi.org/10.1016/j.energy.2020.117440.

[24] Yang H, You P, Shang C. Distributed planning of electricity and natural gas networks and energy hubs. Appl Energy 2021;282:116090. https://doi.org/10.1016/j.apenergy.2020.116090.

[25] Zhong W, Yang C, Xie K, Xie S, Zhang Y. ADMM-Based Distributed Auction Mechanism for Energy Hub Scheduling in Smart Buildings. IEEE Access 2018;6:45635–45. https://doi.org/10.1109/ACCESS.2018.2865625.

[26] East S, Cannon M. An ADMM Algorithm for MPC-based Energy Management in Hybrid Electric Vehicles with Nonlinear Losses. Proc. IEEE Conf. Decis. Control, vol. 2018-December, Institute of Electrical and Electronics Engineers Inc.; 2019, p. 2641–6. https://doi.org/10.1109/CDC.2018.8619731.

[27] Yuan Z, Wogrin S, Hesamzadeh MR. Towards the Power Synergy Hub (PSHub): Coordinating the energy dispatch of super grid by modified Benders decomposition. Appl Energy 2017;205:1419–34. https://doi.org/10.1016/j.apenergy.2017.09.086.

[28] Bahmani R, Karimi H, Jadid S. Cooperative energy management of multi-energy hub systems considering demand response programs and ice storage. Int J Electr Power Energy Syst 2021;130:106904. https://doi.org/10.1016/j.ijepes.2021.106904.

[29] Amir Mansouri S, Javadi MS, Ahmarinejad A, Nematbakhsh E, Zare A, Catalão JPS. A coordinated energy management framework for industrial, residential and commercial energy hubs considering demand response programs. Sustain Energy Technol Assessments 2021;47:101376. https://doi.org/10.1016/j.seta.2021.101376.

[30] Javadi MS, Esmaeel Nezhad A, Siano P, Shafie-khah M, Catalão JPS. Shunt capacitor placement in radial distribution networks considering switching transients decision making

approach. Int J Electr Power Energy Syst 2017;92. https://doi.org/10.1016/j.ijepes.2017.05.001.

[31] Haider ZM, Mehmood KK, Khan SU, Khan MO, Wadood A, Rhee SB. Optimal Management of a Distribution Feeder during Contingency and Overload Conditions by Harnessing the Flexibility of Smart Loads. IEEE Access 2021;9:40124–39. https://doi.org/10.1109/ACCESS.2021.3064895.

[32] Javadi, Sadegh M, Lotfi M, Nezhad AE, Anvari-Moghaddam A, Guerrero JM, et al. Optimal Operation of Energy Hubs Considering Uncertainties and Different Time Resolutions. IEEE Trans. Ind. Appl., vol. 56, Institute of Electrical and Electronics Engineers Inc.; 2020, p. 5543–52. https://doi.org/10.1109/TIA.2020.3000707.

[33] Estahbanati MJ. Hybrid probabilistic-harmony search algorithm methodology in generation scheduling problem. J Exp Theor Artif Intell 2014;26:283–96. https://doi.org/10.1080/0952813X.2013.861876.

[34] Javadi MS, Firuzi K, Rezanejad M, Lotfi M, Gough M, Catalao JPS. Optimal Sizing and Siting of Electrical Energy Storage Devices for Smart Grids Considering Time-of-Use Programs. IECON Proc. (Industrial Electron. Conf., vol. 2019- October, IEEE Computer Society; 2019, p. 4157–62. https://doi.org/10.1109/IECON.2019.8927263.

[35] Javadi MS, Lotfi M, Gough M, Nezhad AE, Santos SF, Catalao JPS. Optimal Spinning Reserve Allocation in Presence of Electrical Storage and Renewable Energy Sources. 2019 IEEE Int Conf Environ Electr Eng 2019 IEEE Ind Commer Power Syst Eur (EEEIC / I&CPS Eur 2019:1–6. https://doi.org/10.1109/EEEIC.2019.8783696.

[36] Ghalelou AN, Fakhri AP, Nojavan S, Majidi M, Hatami H. A stochastic self-scheduling program for compressed air energy storage (CAES) of renewable energy sources (RESs) based on a demand response mechanism. Energy Convers Manag 2016;120:388–96. https://doi.org/10.1016/j.enconman.2016.04.082.